Optimization of Narrow Band-Gap Propylenedioxythiophene:Cyanovinylene Copolymers for Optoelectronic Applications

Emilie M. Galand,[†] Young-Gi Kim,[†] Jeremiah K. Mwaura,[†] Adolphus G. Jones,[†] Tracy D. McCarley,[‡] Vishal Shrotriya,[§] Yang Yang,[§] and John R. Reynolds*,[†]

The George and Josephine Butler Polymer Research Laboratory, Department of Chemistry, Center for Macromolecular Science and Engineering, University of Florida, Gainesville, Florida 32611, Department of Chemistry, Louisiana State University, Baton Rouge, Louisiana 70803, and Department of Materials Science & Engineering, University of California, Los Angeles, California 90095

Received August 21, 2006; Revised Manuscript Received October 11, 2006

ABSTRACT: Four analogues of the narrow band gap poly(3,4-propylenedioxythiophenedialkyl)cyano-*p*-phenylenevinylene (PProDOT−R_2:CNPPV) polymer family have been designed with the goal of improving the film forming ability and utility of this family of polymers when applied in redox switchable and optoelectronic devices. These polymers were synthesized via Knoevenagel condensation with yields ranging from 40 to 80%. Number-average molecular weights between 9000 and 24 000 g mol^{-1} were estimated using size exclusion chromatography, and the polymer repeat unit structures and end groups were confirmed by MALDI mass spectrometry. Linear and branched alkoxy substituents were introduced along the polymer backbone to yield materials highly soluble in chloroform, THF, and toluene, and homogeneous films were prepared by spin-coating or spray-casting from organic solutions. The identity of the substituents has a significant effect on the optical properties of the polymer solutions. A blue-shift in the absorption was observed by replacing linear alkoxy substituents with branched substituents suggesting poorer packing. The HOMO and LUMO energy levels were studied by thin film electrochemistry, and optical band gaps of 1.70−1.75 eV have been determined spectroelectrochemically from the onset of the π to π^* transition, importantly near the wavelength of maximum solar photon flux. These narrow band gap polymers have shown significant photovoltaic performance as electron donors when combined with the electron acceptor [6, 6]-phenyl C_{61}-butyric acid methyl ester (PCBM) in bulk heterojunction photovoltaic devices. AM1.5 efficiencies up to ∼0.4% were attained with short circuit current densities >1.0 mA cm^{-2}, an open circuit voltage of ∼0.7 V, and a fill factor of ∼40%. The identity of the substituents did not have a significant influence on the solubility of the polymers (the linear and branched polymers exhibit a solubility of about 15 mg mL^{-1} in chloroform) and on the films homogeneity. The solubility and film properties of the polymers along with their electrochromic behavior, switching from a neutral blue/purple state to highly transmissive gray in the oxidized and reduced states, are potentially useful in large area electrochromic displays. Polymer light-emitting diodes have been prepared with one of the polymers, exhibiting a bright red emission with $\lambda_{max} = 704$ nm.

Introduction

Intensive research applying conjugated polymers in organic photovoltaic devices,[1−4] polymer light-emitting diodes (PLEDs),[5−7] electrochromic devices,[8−11] and thin-film transistors[12,13] is underway. The development of organic soluble electroactive polymeric materials has been of particular interest for industrial manufacture of large area and flexible devices using techniques such as spray-casting,[14] screen-printing,[15] and inkjet-printing.[16,17] Also, the synthetic flexibility of conjugated polymers allows manipulation of the polymer structure and access to a broad range of optical, electrochemical and physical properties.[18−21]

Organic soluble narrow band gap polymers are particularly desirable for photovoltaics due to their spectral absorption which matches the solar terrestrial radiation.[22−25] They are also needed for deep red and near-IR emitting devices,[22] for applications using n- and p-type conductors,[26] and for electrochromic devices especially due to their potentially multicolored states.[27,28] The donor−acceptor approach (D−A) is one of the most effective ways of building a narrow band gap polymer. The high-lying HOMO of a donor fragment combined with the low-lying LUMO of an acceptor gives rise to a $-(D-A)_x-$ repeat unit structure with an unusually small HOMO−LUMO separation and narrow band gap. [20,29,30]

Significant effort has been applied to the combination of electron rich heterocycles with highly electron demanding cyano-substituted aryl units.[29,31,32] Recently, our group described the synthesis of narrow band gap cyanovinylene−dioxythiophene polymers and the concepts for building an ideal light absorbing material for effective charge transfer to PCBM.[33,34] Specifically, the materials should have (1) a band gap capable of strongly absorbing sunlight ($E_g < 1.8$ eV),[35,36] (2) be resistant to oxidation and consequently have a fairly low lying HOMO (about 5.2 eV or lower,[37] assuming that the energy level of the saturated calomel electrode (SCE) is 4.7 eV below the vacuum level[38]), and (3) should also have a LUMO offset of about 0.3−0.4 eV relative to PCBM[39] for effective charge transfer (above 3.8 eV). In that study, we demonstrated that PProDOT−Hex_2:CNPPV is a promising candidate of the cyanovinylene−

* Corresponding author. E-mail: reynolds@chem.ufl.edu.
[†] The George and Josephine Butler Polymer Research Laboratory, Department of Chemistry, Center for Macromolecular Science and Engineering, University of Florida.
[‡] Department of Chemistry, Louisiana State University.
[§] Department of Materials Science & Engineering, University of California, Los Angeles.

10.1021/ma061935o CCC: $33.50
Published on Web 12/19/2006

Scheme 1

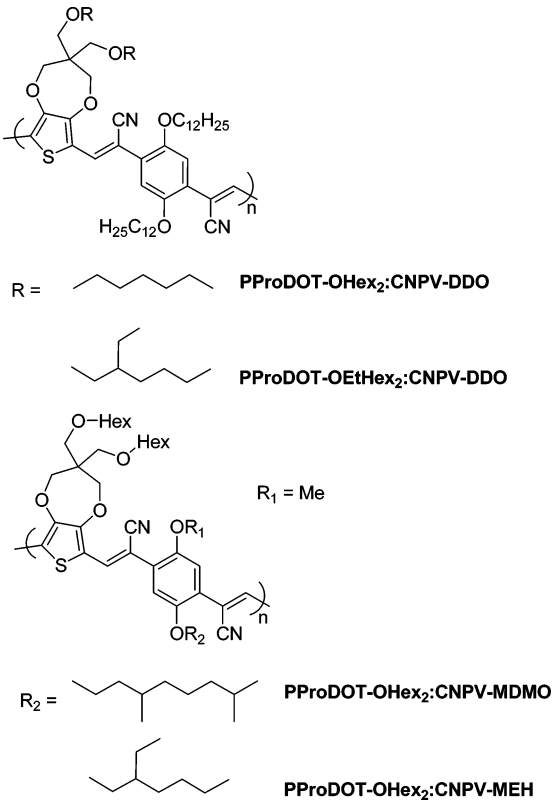

dioxythiophene family for photovoltaic devices. It is a strongly absorbing photoexcitable donor for PCBM, and exhibits good solubility, an optical band gap of 1.7 eV, a HOMO level of 5.7 eV and a LUMO level of 3.5 eV. However, initial observations have shown that spin-coated films of the polymer blended with poly(2-methoxy-5-(2′-ethylhexyloxy)-1,4-phenylenevinylene) (MEH−PPV) and with the acceptor PCBM, have a discontinuous surface which becomes rougher as the contents of PProDOT−Hex_2:CNPPV increase, probably due to an aggregated polymer morphology. Photovoltaic efficiencies of 0.1−0.2% have been measured, suggesting the need of further polymer structural optimization. In parallel with the photovoltaic study, it has also been observed that this polymer provides appealing electrochromic properties, switching between a deep blue neutral state and colorless transmissive reduced and oxidized states. Finally, it is important to note that this polymer is synthesized by Knoevenagel polymerization and does not involve the use of transition metal catalysts. Catalyst impurities are often trapped in the polymer and are responsible for photoluminescence quenching, electrical shorts or preferred conduction paths in thin film devices leading to decreased performance.[40]

In pursuit of enhanced processing for photovoltaics and to further investigate the electrochromic capabilities of propylenedioxythiophene:cyanovinylene polymers, we decided to synthesize analogues of PProDOT−Hex_2:CNPPV and study a variety of side chains as shown in Scheme 1. The effects of the side chains on the optical and electronic properties, solubility, and film forming ability were studied. Specifically, we report on the substitution of the ProDOT moieties with alkoxy chains to attain higher solubility and greater processability relative to the alkyl substituted PProDOT−Hex_2:CNPPV polymer.[33] The first polymer, PProDOT−$OHex_2$:CNPV−DDO, was fully substituted with linear alkoxy substituents: linear dodecyloxy chains on the phenylene ring and linear hexyloxy chains on the ProDOT ring as illustrated in Scheme 1. Disorder inducing branches were

Scheme 2

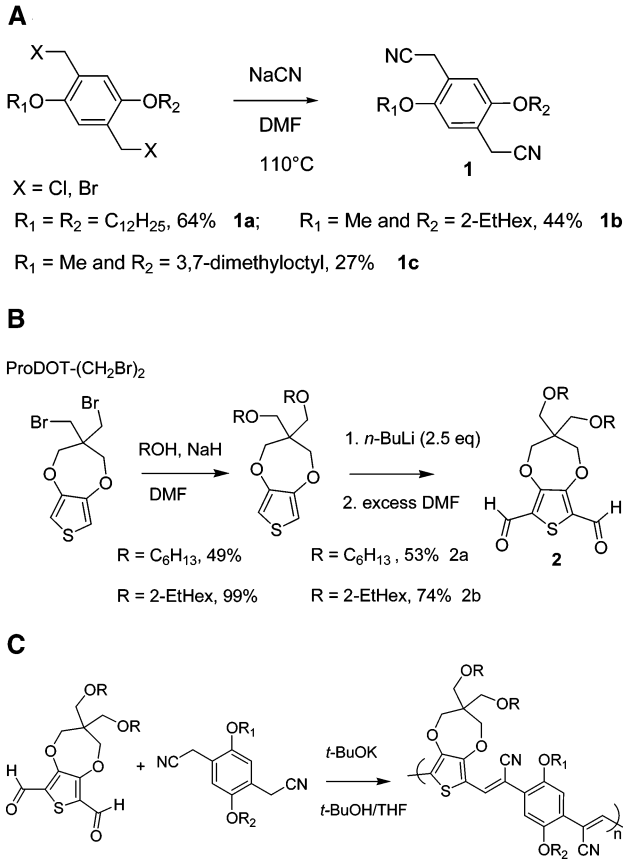

introduced on the ProDOT moiety of the second polymer, PProDOT−$OEtHex_2$:CNPV−DDO, this material being also substituted with linear dodecyloxy substituents on the phenylene ring but with 2-ethylhexyloxy chains on the ProDOT ring. The branching location was changed on the third and fourth polymers by using linear hexyloxy chains on the ProDOT ring and unsymmetrically substituting the phenylene ring with methyloxy groups and 2-ethylhexyloxy (PProDOT−$OHex_2$:CNPV−MEH)) or 3,7-dimethyloctyloxy groups (PProDOT−$OHex_2$:CNPV−MDMO). Also, with PProDOT−$OHex_2$:CNPV−MEH and PProDOT−$OHex_2$:CNPV−MDMO we considered substitution mimicking those in MEH−PPV and poly(2-methoxy-5-(3,7-dimethyloctyloxy)-1,4-phenylenevinylene) (MDMO−PPV), the most efficient polymers to date for organic solar cells[41,42] [along with poly(3-hexylthiophene)].

Molecular and macromolecular characterization was accomplished by a combination of NMR and IR spectroscopy, MALDI mass spectrometry, and GPC. ^{1}H NMR and IR spectroscopy confirmed the polymerization with the disappearance of monomer peaks, while MALDI mass spectrometry confirmed the polymer structure with a spacing between the peaks corresponding to two repeat units of the polymers and residual masses of 18 Da. Number-average molecular weights ranging from 9000 to 24 000 g mol^{-1} have been estimated by GPC relative to polystyrene standards. The polymers are soluble in organic solvents (∼15 mg mL^{-1} in chloroform) affording the deposition of polymeric thin-films onto working electrodes via spray-casting and spin-coating for the study of the spectroelectrochemical and redox properties. An exploration of the polymers electrochromic properties, light-emitting capacities, and light-harvesting properties in bulk heterojunction polymer/PCBM solar cells is included.

Table 1. GPC Estimated Molecular Weights of the Copolymers (Polystyrene Standards, THF as Mobile Phase) and Yields of the Knoevenagel Polymerizations

	M_n (g mol^{-1})	M_w (g mol^{-1})	PDI	avg. no. of rings	yield (%)
PProDOT−OEtHex$_2$:CNPV−DDO	10 300	14 800	1.4	20	61
PProDOT−OHex$_2$:CNPV−DDO	13 000	17 500	1.3	28	77
PProDOT−OHex$_2$:CNPV−MEH	23 700	31 100	1.3	66	45
PProDOT−OHex$_2$:CNPV−MDMO	8700	11 400	1.3	22	41

Results and Discussion

Monomer and Polymer Synthesis. The synthesis of the acetonitrile monomers (**1**) was previously reported in the literature,[43−45] and only the final step illustrating all the derivatives of concern is shown in Scheme 2A. The ProDOT moieties were derivatized with linear and branched alkoxy chains using nucleophilic substitution of the corresponding alcohols on the key ProDOT($CH_2Br)_2$ precursor previously synthesized by our group[8] (see Scheme 2B). Lithiation with *n*-butyllithium followed by addition of excess DMF afforded the dialdehyde monomers (**2**).

The polymerization was accomplished by Knoevenagel condensation of the acetonitrile and aldehyde monomers in a 1:1 mixture of *t*-BuOH/THF with 1 equiv of *t*-BuOK per cyano group as shown in Scheme 2C. After a 2 h reflux, the polymers were precipitated into methanol and filtered into a cellulose extraction thimble. The thimble was placed in a Soxhlet apparatus and methanol was refluxed over the thimble for 24 h to remove any unreacted monomer and base. Final extraction with chloroform afforded blue or purple solids in yields ranging between 40 and 80% after solvent evaporation (see Table 1).

The polymers are soluble in common organic solvents such as hexanes, chloroform, methylene chloride and tetrahydrofuran (about 15 mg mL^{-1} in chloroform). ^{1}H NMR, IR, and MALDI mass spectrometry support the proposed structures of the polymers. End groups were not visible by ^{1}H NMR. Residual nitrile IR stretching bands at $\sim$ 2250 cm^{-1} corresponding to the monomers were not observed, while bands were observed at $\sim$ 2204 cm^{-1} indicating the presence of conjugated cyanovinylene linkages (shown in the Supporting Information for PProDOT−OEtHex$_2$:CNPV−DDO). MALDI analyses performed with a HABA matrix confirm the polymer structure with a spacing between the peaks corresponding interestingly to the molecular weight of two repeat units. This phenomenon has already been observed for PProDOT−Hex$_2$:CNPPV[34,46] and, as illustrated by the results of Figure 1, only even-numbered chains are seen in the MALDI spectra (see Supporting Information). This effect has been observed in polycondensation reactions and has been explained by the cyclization of the polymer chains due to strong electronic interactions (e.g. $\pi-\pi$, donor−acceptor, and dipole−dipole interactions) enforcing a parallel and coplanar alignment of the growing chains, inducing a hairpin conformation.[47,48] On the basis of the observed *m*/*z* values for the polymers and the mass accuracy of our instrument, we are able to identify the oligomers as linear species and rule out the possibility that they are cyclic. In fact, the observed residual mass of 18 Da, presumably H_2O, is consistent with end groups of a phenylene unit with a single free acetonitrile and a ProDOT unit with a single free aldehyde.

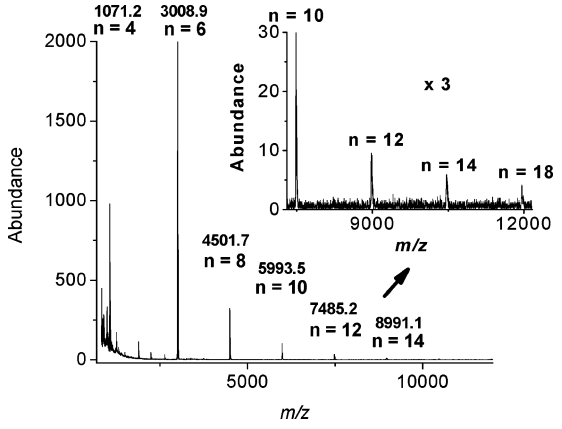

Figure 1. MALDI MS of PProDOT−OHex$_2$:CNPV−MDMO illustrating that the dominant spacing pattern corresponds to two repeat units. HABA was used as the matrix. The inset is a 3× magnification of the 5000−12 000 *m*/*z* region.

Molecular Weight Characterization. Molecular weight analyses performed by GPC (polystyrene standards, THF as mobile phase) gave number-average molecular weights ranging from 9000 to 24 000 g mol^{-1} which corresponds to an average number of rings ranging from 20 to 66 per chain (see Table 1). The use of stoichiometric proportions of acetonitrile and aldehyde monomers is a necessity in this A−A + B−B polycondensation. This is made difficult by the aldehyde monomers **2** being sticky oils, which makes accurate weighing difficult. This may explain the variation in the molecular weights obtained, and we suppose that near stoichiometric conditions were reached for the synthesis of PProDOT−OHex$_2$:CNPV−MEH, which exhibits the highest molecular weight of about 24 000 g mol^{-1}. MALDI analysis confirmed the presence of chains up to 12−18 repeat units (vide ante and Supporting Information), though no conclusion can be given on the average molecular weights using this method since it is more difficult for high molecular weight mass components to undergo the desorption/ionization process, "fly" in the mass spectrometer and be detected.[49−51]

As illustrated in Figure 2 for PProDOT−OEtHex$_2$:CNPV−DDO and in the Supporting Information section for the other polymers, chromatographic polymer elution during GPC analysis was monitored with an in-line photodiode array detector to record the UV−vis absorption of selected fractions of the polymers. Spectra were recorded at various elution times which

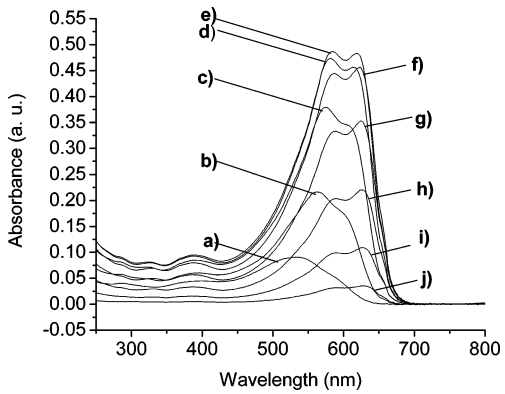

Figure 2. Absorption spectra for molecular weight fractions of PProDOT−OEtHex$_2$:CNPV−DDO. Absorption maxima (λ_{max}) and molecular weights in g mol^{-1} vs polystyrene are reported: (a) 534.1 nm, 5000; (b) 562.1 nm, 6500; (c) 574.3 nm, 8900; (d) 581 and 612 nm, 12 200; (e) 582.8 and 617.1 nm, 15 100; (f) 623.2 nm, 20 000; (g) 624.4 nm, 27 000; (h) 626.8 nm, 36 000; (i) 626.8 nm, 49 300; (j) 626.8 nm, 69 500.

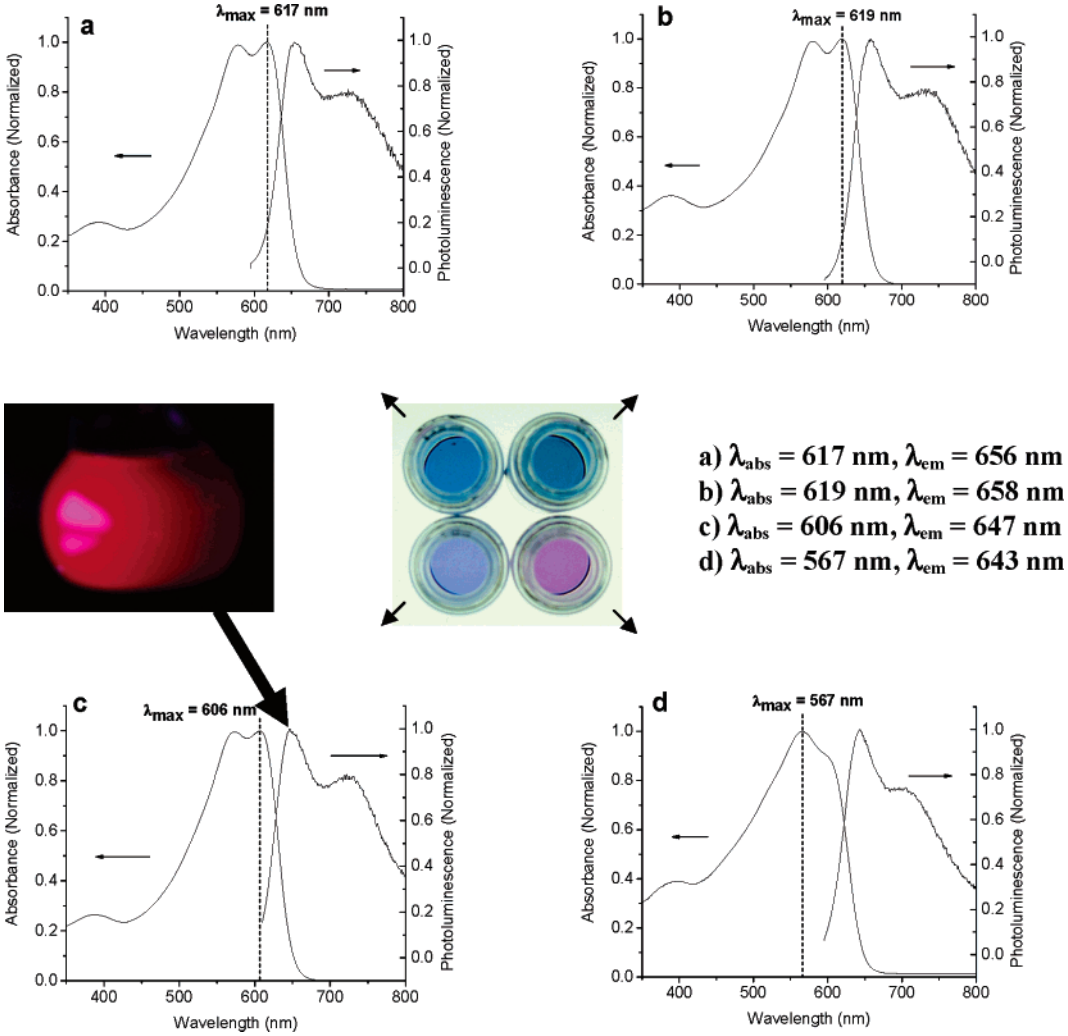

Figure 3. Solution UV−vis absorbance and photoluminescence of polymers in toluene: (a) PProDOT−OEtHex$_2$:CNPV−DDO; (b) PProDOT−OHex$_2$:CNPV−DDO; (c) PProDOT−OHex$_2$:CNPV−MEH; (d) PProDOT−OHex$_2$:CNPV−MDMO. The photograph in the center illustrates the colors of toluene solutions of the different polymers and the left photograph illustrates the photoluminescence of PProDOT−OHex$_2$:CNPV−MEH irradiated by UV light.

allowed monitoring polymer absorption as a function of molecular weight relative to the polystyrene standards. The polymers exhibit a broad absorption in the 500−700 nm visible region. For PProDOT−OEtHex$_2$:CNPV−DDO we begin reaching the polymer limit when the molecular weight reaches about 12 000 g mol^{-1} (Figure 2d). Below that molecular weight, the absorption spectra exhibit maxima centered in the 530−580 nm region and a broad shoulder around 620 nm; above 12 000 g mol^{-1}, the shoulder becomes more defined giving rise to a second absorption maximum undergoing small changes from 617 to 627 nm as the chain size further increases. For PProDOT−OHex$_2$:CNPV−DDO, PProDOT−OHex$_2$:CNPV−MEH, and PProDOT−OHex$_2$:CNPV−MDMO the polymer limits were reached after about 15 000, 20 000, and 12 000 g mol^{-1} respectively, since little variations in the absorption maxima were observed at higher molecular weights (see Supporting Information). The comparison between these results and the number-average molecular weights summarized in Table 1 supports that our polymers have desirable degrees of polymerization and dispersity.

Thermal Properties. The thermal stability of the polymers was studied by thermogravimetric analysis (TGA) in a nitrogen atmosphere using a 20 °C min^{-1} temperature ramp from 50 to 900 °C. The thermograms show that the polymers exhibit a high thermal stability losing less than 2−3% weight at 300 °C followed by a drastic degradation process at about 370 °C. Above 800 °C less than 20% of material remains (see Supporting Information).

Polymer Solution Optical Properties. Figure 3 shows the solution UV−vis absorbance and photoluminescence of the polymers in toluene. They absorb over a broad spectral range (ca. 500−700 nm), with absorption coefficients[35] around 25 000 M^{-1} cm^{-1}. The polymer substituted with linear chains on the phenylene and ProDOT rings (PProDOT−OHex$_2$:CNPV−DDO, Figure 3b) exhibits an absorption maximum at 619 nm and the polymer solution is deep blue. As we introduce branches on the ProDOT ring (PProDOT−OEtHex$_2$:CNPV−DDO, Figure 3a) the absorption maximum changes a little to 617 nm, while it drastically falls to 606 nm (PProDOT−OHex$_2$:CNPV−MEH, Figure 3c) as branches are introduced on the phenylene moiety, and the solution color becomes more red as demonstrated in the photographs in Figure 3. A λ_{max} of 567 nm is observed for PProDOT−OHex$_2$:CNPV−MDMO as the vibronic coupling which yields splitting in the spectrum is reduced. Unsymmetrical branching on the phenylene ring induces a large influence on the polymer disorder and conjugation, shifting the absorption to the blue region, transmitting more red light and giving the solution a purple appearance, whereas branching on the ProDOT unit seems to have no significant influence. The polymers emit in the red and near-infrared region with emission maxima

Table 2. Summary of Thin Film Polymer Electrochemistry, and HOMO and LUMO Energies of the Polymers Derived from the Electrochemical Results

polymer	$E_{onset,ox}$ CV (V)	HOMO CV (eV)	$E_{onset,red}$ CV (V)	LUMO CV (eV)	$E_{onset,ox}$ DPV (V)	HOMO DPV (eV)	$E_{onset,red}$ DPV (V)	LUMO DPV (eV)	$E_{g,opt}$ (eV)
PProDOT−OEtHex$_2$:CNPV−DDO	0.8	5.9	−1.5	3.6	0.6	5.7	−1.5	3.6	1.75
PProDOT−OHex$_2$:CNPV−DDO	0.8	5.9	−1.6	3.5	0.6	5.7	−1.5	3.6	1.70
PProDOT−OHex$_2$:CNPV−MEH	0.6	5.7	−1.5	3.6	0.6	5.7	−1.4	3.7	1.70
PProDOT−Hex$_2$:CNPV−MDMO	0.7	5.8	−1.5	3.6	0.6	5.7	−1.5	3.6	1.75

decreasing from 658 nm for the more ordered polymer (Figure 3b) to 643 nm for the least ordered polymer (Figure 3d), as illustrated for PProDOT−OHex$_2$:CNPV−MEH in the photograph in Figure 3c. The fluorescence quantum efficiency of the polymers was estimated around 12% (Oxazine 1 standard; $\Phi = 0.11$).[52]

Polymer Electrochemistry. For photovoltaic, electrochromic or LED applications it is necessary to have a good understanding of the redox properties of the polymers and to be able to estimate the HOMO and LUMO levels. Toward that end, cyclic voltammetry (CV) and differential pulse voltammetry (DPV) were employed. Polymer films were deposited by drop-casting on a Pt button electrode from a 5 mg mL^{-1} chloroform solution, and the voltammograms were recorded in 0.1 M tetra-*n*-butylammonium hexafluorophosphate ($TBAPF_6$) in acetonitrile (ACN) electrolyte. The measurements were performed in an oxygen and water free environment in an argon-filled glovebox due to the instability of the reduced form of the polymers.[37] The oxidation and reduction processes were addressed separately as cycling over the full potential range resulted in rapid polymer degradation. Multiple cycling was used to break in the polymers, and the measurements were taken once the electrochemical response became constant.

Figure 4 shows the CV and DPV results obtained for PProDOT−OEtHex$_2$:CNPV−DDO; the results for the other polymers can be found in the Supporting Information. The polymers exhibit onsets of oxidation ranging from 0.6 to 0.8 V vs Fc/Fc$^+$ (all further potentials will be reported vs this reference electrode) and onsets of reduction ranging from −1.4 to −1.6 V as detailed in Table 2. The differences between the oxidation and reduction potentials yield electrochemical band gaps varying between 2.0 and 2.4 eV, with the band gaps obtained by DPV being slightly smaller than those obtained by CV. This is not surprising since the onsets of oxidation measured by DPV are generally more defined than those obtained by CV. Indeed, DPV measures a current difference and the major component of that difference is the faradaic current. The capacitive component due to the charging of the electrode double layer is largely eliminated in comparison with CV measurements. DPV also avoids prepeaks that are observed for instance on the CV spectrum of PProDOT−OHex$_2$:CNPV−MDMO (see Supporting Information) and which are attributed to trapped charges in the polymer film.[20] The polymer HOMO and LUMO energies were estimated from the onsets of oxidation and reduction, respectively. The polymers are relatively stable to oxidation with low lying HOMO levels varying between 5.7 and 5.9 eV (assuming that the half wave potential of ferrocene (Fc/Fc$^+$) = 0.38 V vs SCE[53]). These low HOMO values allow the polymers to be easily handled in air without encountering undesired oxidation. This is a useful property as we consider use of these materials in optoelectronic devices. With LUMO levels around 3.5−3.7 eV the polymers are also good candidates for charge transfer to C_{60}-based acceptors (0.5−0.7 eV LUMO offsets with LUMO of PCBM being at 4.2 eV). These results are in accordance with those previously reported on the PProDOT−Hex$_2$−CNPPV analogue.[33,34,46]

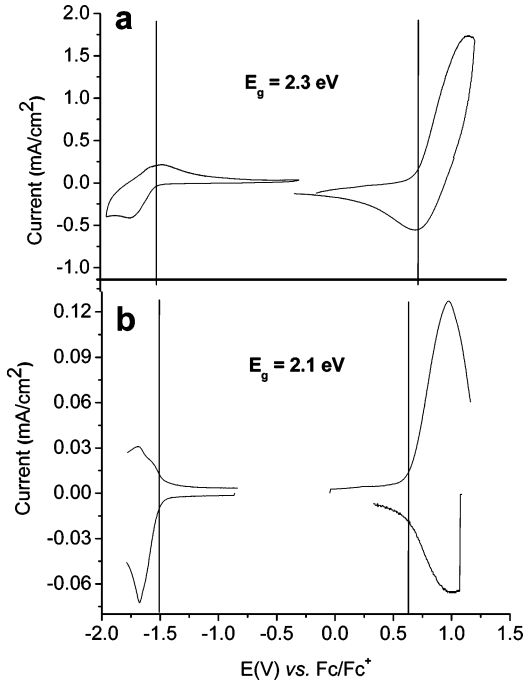

Figure 4. Polymer cyclic voltammetry (CV) and differential pulse voltammetry (DPV): (a) CV of PProDOT−OEtHex$_2$:CNPV−DDO; (b) DPV of PProDOT−OEtHex$_2$:CNPV−DDO. Measurements were performed on a 0.02 cm^2 Pt button working electrode in 0.1 M $TBAPF_6$/acetonitrile with a Pt foil counter electrode and a silver wire pseudo reference electrode calibrated vs Fc/Fc$^+$.

Polymer Spectroelectrochemistry. Spectroelectrochemical measurements were performed in order to define the optical band gaps of the polymers and observe their spectral response to doping. Homogeneous and high quality polymer films were produced by spray casting polymer solutions (5 mg mL^{-1} in chloroform) onto ITO coated glass using an air brush at 12 psi. The spectral changes upon oxidation were recorded in 0.1 M TBAP/propylene carbonate electrolyte as illustrated in Figure 5. In the neutral state, the polymers absorb across the entire visible region, exhibiting deep blue or purple (for PProDOT−OHex$_2$:CNPV−MDMO) colors, and optical band gaps of 1.70−1.75 eV were calculated from the onset of the $\pi-\pi^*$ transition, right at the solar radiation maximum. These values are lower than the electrochemical values and such disagreements have been previously reported for cyanovinylene polymers.[20,34] For photovoltaic applications, determination of the band gaps is best done using the spectroscopic results for correlation to solar light absorption. The polymer films were progressively oxidized by applying increasing positive potentials in 50 mV steps. Near the onset potential for oxidation, the $\pi-\pi^*$ transition of the neutral state started to decrease in intensity and lower energy charge carrier associated peaks started to grow in the near-IR region changing the film color to a transmissive light gray. It is interesting to note that these electrochromic properties are comparable to PEDOT which is most generally studied from electrochemically formed films, or from films prepared by casting/spin-coating of PEDOT−PSS. At the same time, these

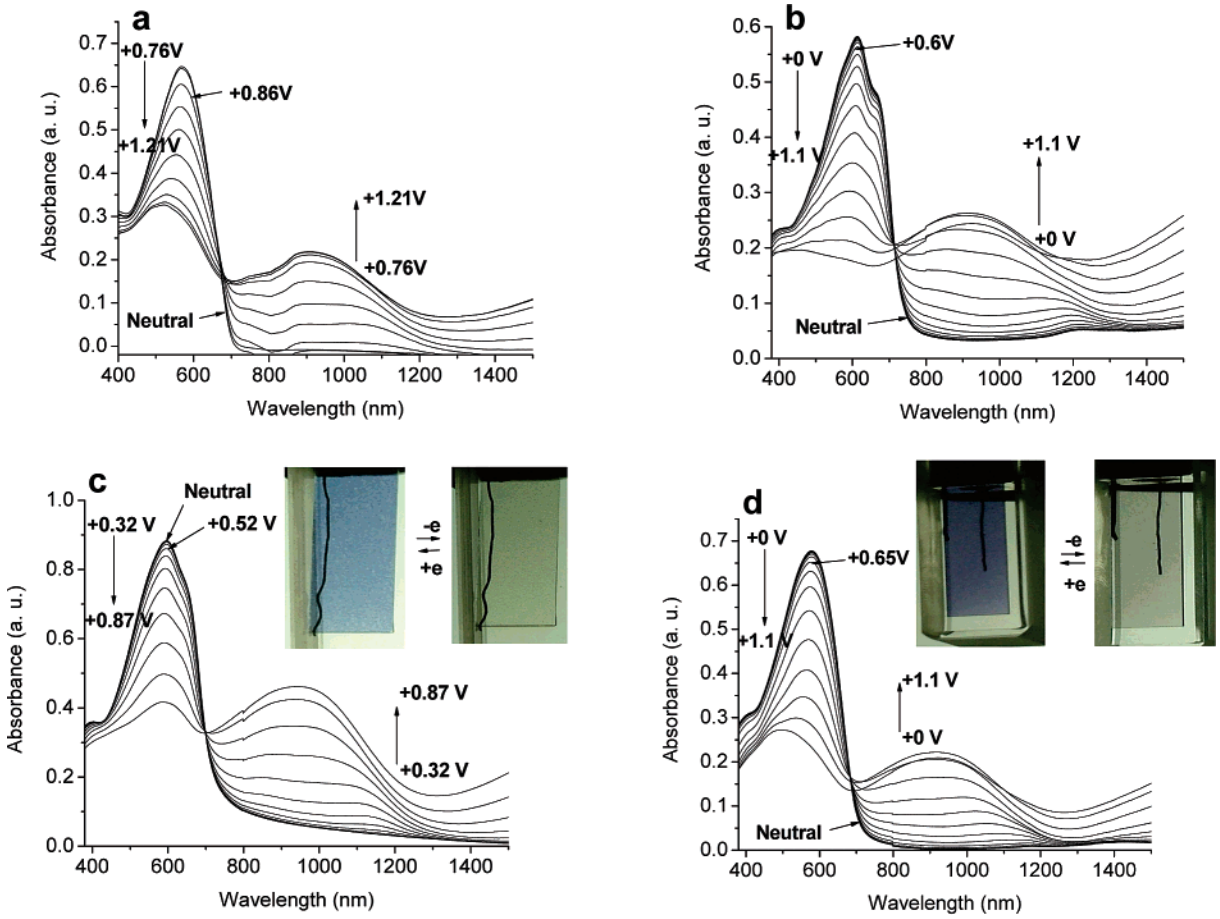

Figure 5. Oxidative spectroelectrochemistry of polymers: (a) PProDOT−OEtHex$_2$:CNPV−DDO; (b) PProDOT−OHex$_2$:CNPV−DDO; (c) PProDOT−OHex$_2$:CNPV−MEH; (d) PProDOT−OHex$_2$:CNPV−MDMO. Polymer films were spray cast from chloroform solution on ITO coated glass. All potentials are reported vs Fc/Fc$^+$. The supporting electrolyte consisted of 0.1 M TBAP/propylene carbonate. The potential was increased in 50 mV steps.

organic soluble and processed polymers are more stable in their neutral forms allowing easy handling.

The spectral changes were also recorded upon reduction in 0.1 M TBAPF$_6$/ACN electrolyte as illustrated in Figure 6. As for the CV and DPV measurements, these studies have been performed in an oxygen and water free environment. The polymer films were progressively reduced by applying increasing negative potentials in 100 mV steps. As the potentials reach the onset of reduction observed by electrochemistry (for instance between −1.5 and −1.6 V for PProDOT−OHex$_2$:CNPV−MEH), the $\pi-\pi^*$ transition of the neutral state decreases in intensity and lower energy charge carrier associated peaks evolve in the near-IR region changing the film color to transmissive light gray, as was also observed for the oxidation process.

Colorimetry. Polymer films were deposited on ITO by spray-casting from 5 mg mL^{-1} chloroform solutions and were analyzed by in-situ colorimetric analysis using 0.1 M TBAP/propylene carbonate as the supporting electrolyte. The relative luminance (the brightness of the transmitted light as a percentage of the brightness of the light source) was measured as the polymers were progressively oxidized.[54] This experiment follows changes in light transmission with doping level. Optical changes again occur once the potentials reach the electrochemical onsets of oxidation as illustrated in Figure 7. For instance, the onset of oxidation measured by CV for PProDOT−OEtHex$_2$:CNPV−DDO is at 0.8 V (Table 2) and the relative luminance starts increasing around this value. In the neutral state, the polymer films are quite opaque and colored, with a relative luminance varying between 27 and 37%. In the fully oxidized state, the films become highly transmissive, with luminance values ranging from 65 to 82%, and a relative luminance change up to 50% was observed for PProDOT−OHex$_2$:CNPV−MEH, which is useful for electrochromic applications. The $L^*a^*b^*$ values of the colors were also determined to allow color matching, and the results are summarized in Table 3 along with the corresponding colors in the neutral and oxidized states.

Polymer Electroluminescent Properties. As is shown in Figure 3c, the polymers exhibit a red fluorescence in toluene. The thin-film photoluminescence (PL) spectrum shown in Figure 8 for PProDOT−OHex$_2$:CNPV−MEH has a shape to that of the solution photoluminescence, although it is red shifted due to the more organized conformation expected in the solid state. To evaluate the polymers potential utility in light-emitting diodes (LEDs), devices were prepared with the following architecture: ITO/PEDOT−PSS (40 nm)/ PProDOT−OHex$_2$:CNPV−MEH (50 nm)/Ca (5 nm)/Al (200 nm). As illustrated by the dotted line spectrum in Figure 8, the device exhibits a broad emission in the red and near-infrared region dominated by a peak at λ_{max} = 704 nm. The bright red color observed is illustrated by the photograph in Figure 8. The electroluminescence (EL) spectrum is similar to the PL spectrum of the solid film (Figure 8), indicating that the EL results from a singlet $\pi-\pi^*$ exciton with the same structure as that produced by photoexcitation. Figure 9 shows the device characteristics, especially a turn-on voltage of 4 V and an EL intensity which increases with voltage up to 10 V. We note that the radiance decreases at higher voltages possibly due to device breakdown.

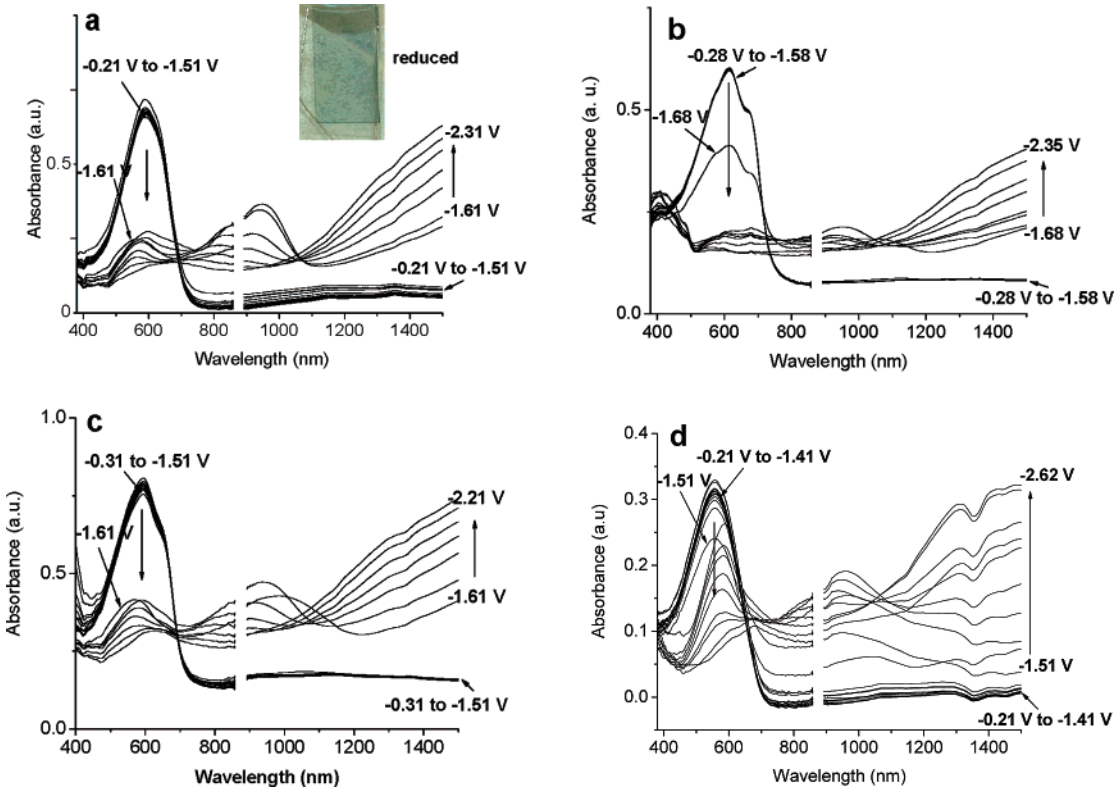

Figure 6. Reductive spectroelectrochemistry of polymers: (a) PProDOT−OEtHex$_2$:CNPV−DDO; (b) PProDOT−OHex$_2$:CNPV−DDO; (c) PProDOT−OHex$_2$:CNPV−MEH; (d) PProDOT−OHex$_2$:CNPV−MDMO. Polymer films were spray cast from chloroform solution on ITO coated glass. All potentials are reported vs Fc/Fc$^+$. The supporting electrolyte consisted of 0.1 M TBAPF$_6$/acetonitrile. The potential was increased in 0.1 V steps. No data is shown between 860 and 890 nm as the detectors do not cover this wavelength range.

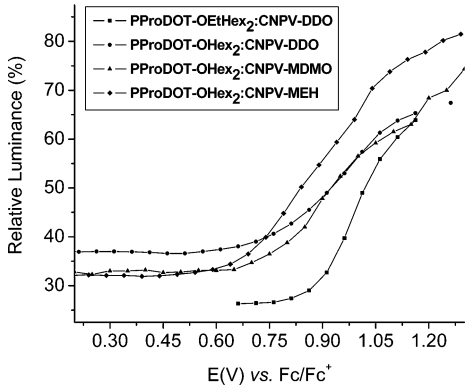

Figure 7. Relative luminance (%) as a function of applied potential for every polymer. Polymer films were spray cast from chloroform solution on ITO coated glass (5 mg mL^{-1}). The supporting electrolyte consisted of 0.1 M TBAP/propylene carbonate.

At 10 V, the device emits its highest luminance at ~77 μW cm^{-2} sr (526 cd m^{-2}) and current density of 1556 mA cm^{-2}. Unfortunately, the external electron-to-photon quantum efficiency was determined to be low and it has been concluded that the polymer is not likely effective for development in LED applications.

Photovoltaic Devices. It was previously reported that the PProDOT−Hex$_2$:CNPPV analogue of our polymers can transfer electrons to PCBM upon photoexcitation.[33,46] This conclusion was based on PL quenching experiments showing that 95% of the PL was quenched in thin films blends with PCBM, and on IPCE measurements of PProDOT−Hex$_2$:CNPPV/PCBM solar cells which indicate that the polymer is the major contributor to the photocurrent in the device.

We prepared bulk heterojunction solar cells using the PProDOT−R$_2$:CNPV polymers as the electron donors and PCBM as the electron acceptor (device structure ITO/PEDOT−PSS/(PProDOT−R$_2$:CNPV/PCBM)/LiF/Al). Blends containing 1:4 (w/w) of each polymer with PCBM were spin-coated from dichlorobenzene solutions and the photoactive layer thickness was kept between 30 and 40 nm. Thicker photoactive layers led to drops in photocurrent density and fill factor, a phenomenon which is attributed to an increase in the series resistance. Figure 10 shows the $i-V$ characteristics of the PProDOT−OHex$_2$:CNPV−MEH based device under AM 1.5 illumination for a calibrated solar simulator with an intensity of 100 mW cm^{-2}. The photovoltaic results obtained for the other polymers are summarized in Table 4. PProDOT−OHex$_2$:CNPV−MEH exhibited the best performance, with a power conversion efficiency (η) of about 0.4%, an open circuit voltage (V_{oc}) of 0.76 V, a short circuit current (I_{sc}) of 1.5 mA cm^{-2} and a fill factor (FF) of 36%. According to the results summarized in Table 4, there is a ~ 0.1−0.27% efficiency range for the other polymers which have lower molecular weights (vide ante). This observation suggests that higher molecular weight materials are likely to enhance the photoinduced current densities in the PCBM solar cells. Independent device fabrication and measurements were conducted in both University of Florida (UF) and University of California (UCLA) laboratories for PProDOT−OEtHex$_2$:CNPV−DDO/PCBM. Very similar power conversion efficiencies of 0.27% vs 0.26% were achieved, supporting the reproducibility of the results.

Incident photon to current efficiency measurements (IPCE) match the polymer absorption spectra near the absorption maximum of the polymers, indicating that the polymers are effective photoexcited electron donors that contribute mainly to the photocurrent in the device (Supporting Information).

Table 3. Colorimetric Results for the Neutral and Oxidized Polymers[a]

polymer film	charge state	E (V)	L	a	b	observed color
PProDOT−OEtHex$_2$:CNPV−DDO	N	0.65	58	1	−35	blue
PProDOT−OEtHex$_2$:CNPV−DDO	O	1.15	84	3	2	gray
PProDOT−OHex$_2$:CNPV−DDO	N	0.45	67	−4	−22	blue
PProDOT−OHex$_2$:CNPV−DDO	O	1.15	85	2	2	gray
PProDOT−OHex$_2$:CNPV−MEH	N	0.45	63	4	−28	blue
PProDOT−OHex$_2$:CNPV−MEH	O	1.15	90	0	5	gray
PProDOT−OHex$_2$:CNPV−MDMO	N	0.45	64	8	−18	purple
PProDOT−OHex$_2$:CNPV−MDMO	O	1.15	83	1	1	gray

[a] Key: N = neutral; O = oxidized.

Table 4. Summarized Photovoltaic Characteristics of Polymer/PCBM Based Solar Cells[a]

polymers	η (%)	FF	V_{oc} (V)	I_{sc} (mA/cm^2)	PAL thickness (nm)
PProDOT−OEtHex$_2$:CNPV−DDO	0.27	0.39	0.65	1.05	30
PProDOT−OHex$_2$:CNPV−DDO	0.1	0.34	0.58	0.5	37
PProDOT−OHex$_2$:CNPV−MEH	0.36	0.37	0.73	1.32	38
PProDOT−OHex$_2$:CNPV−MDMO	0.13	0.28	0.72	0.66	38

[a] Averaged values for three pixels for each polymer.

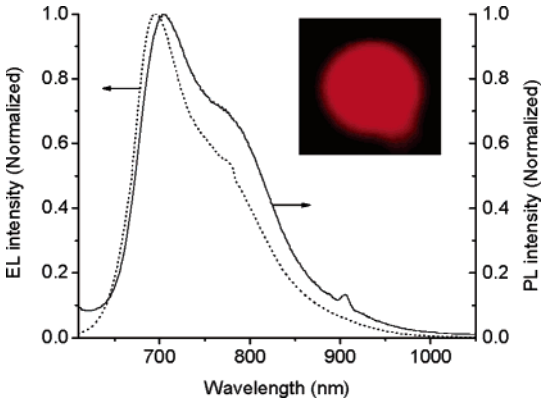

Figure 8. Normalized photoluminescence emission spectrum of PProDOT−OHex$_2$:CNPV−MEH in thin film (solid line) superimposed with normalized electroluminescence spectrum and accompanying photograph of an ITO/PEDOT−PSS/ PProDOT−OHex$_2$:CNPV−MEH/ Ca/Al device (dotted line).

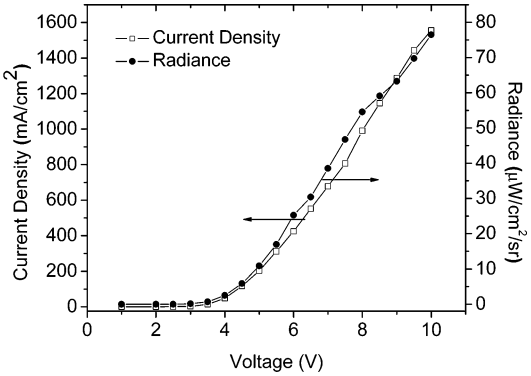

Figure 9. Effect of applied voltage on current density (□) and radiance (●) for an ITO/PEDOT−PSS/ PProDOT−OHex$_2$:CNPV−MEH/Ca/ Al device.

However, the IPCE values are quite low for all the polymers, between 6 and 8% in the 500−590 nm region and below 2% above 680 nm.

Several parameters are suspected to be responsible for the low efficiencies, and disorder is one of them. Disorder in a polymer inhibits hole mobility, which is believed to be the bottleneck for the short circuit current. In addition, when hole mobility is significantly lower than that of the electron mobility in conjugated polymer/PCBM blends, severe space charge effects lead to a poor fill factor. While our light absorption and energy level alignment are nearly optimal, reduced transport

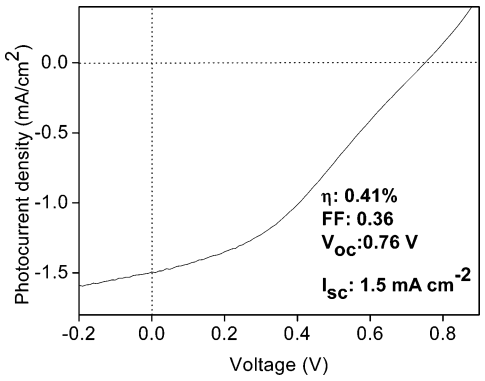

Figure 10. Current voltage characteristic of a solar cell made of a 1/4 blend (w/w) of PProDOT−OHex$_2$:CNPV−MEH/PCBM under AM1.5 conditions (100 mW cm^{-2}).

properties dominate and limit the device performance. Improving carrier mobility in these polymers is of primary importance for device enhancement. For that reason, we are currently performing a full study of the polymers ordering properties (AFM imaging, X-ray, DSC, etc.) and of the effect of annealing on the charge mobility and photovoltaic performance.

Summary and Perspective

This report gives an outlook on how small structural changes on a polymer backbone can affect the solubility, optical, and device properties of a material. PProDOT−Hex$_2$:CNPPV was initially targeted and utilized as a derivative of interest for electrochromics and photovoltaics. Working around its backbone structure and length, we were able to make progress toward improving film quality and photovoltaic properties. The replacement of the alkyl substituents by alkoxy substituents improved solubility without affecting the electronic properties. The highest molecular weight material was more efficient in enhancing the photoinduced current densities. The replacement of the linear substituents by branches does not have a significant influence on the solubility. However, it significantly induced disorder and backbone twisting in solution especially in the polymers containing unsymmetrically substituted phenylene rings, shifting the absorption maxima of the polymer solutions to the blue region. The extent of disorder induced by branches on $\pi-\pi$ stacking and intermolecular charge transport in the solid state is currently under study. The photovoltaic efficiencies are a bit low when compared to those obtained for P3HT/PCBM devices.[55−57] This might be explained by several factors such

as the cyano groups acting as trapping sites for the electrons, and the possibility of a low degree of order. Further structural manipulation and morphological characterization is needed for optimization in solar cells. As was observed for PProDOT−Hex_2:CNPPV, the polymers exhibit appealing electrochromic properties, switching between blue/purple colors in the neutral state and highly transmissive light gray colors in the reduced and oxidized states. These electrochromic properties, along with the improved film forming ability, make these materials of great interest for electrochromic applications involving large and flexible surfaces.

Experimental Section

Materials. All chemicals were purchased from Fisher Scientific and used as received unless stated otherwise. Tetrahydrofuran (THF), *tert*-butyl alcohol, CH_2Cl_2, and CH_3CN were dried and distilled prior to use. Tetrabutylammonium perchlorate (TBAP) was recrystallized from 2-propanol. ProDOT(CH_2Br),[8] 3,3-bis(2-ethylhexyloxymethyl)-3,4-dihydro-2*H*-thieno-[3,4-*b*][1,4]-dioxepine [ProDOT($CH_2OEtHex)_2$],[8] 1,4-bis(bromomethyl)-2,5-bis-(dodecyloxy)benzene,[58] 2,5-bis(bromomethyl)-1-methoxy-4-[(2-ethylhexyl)oxy]benzene,[44] and 1,4-bis(chloromethyl)-2-(3,7-dimethyl-oxy)-5-methoxybenzene[45] were synthesized using known procedures.

1,4-Bis(cyanomethyl)-2,5-bis(dodecyloxy)benzene (1a).[46] Sodium cyanide (1.94 g, 3.95×10^{-2} mol, 2.5 equiv) and 1,4-bis-(bromomethyl)-2,5-bis(dodecyloxy)benzene (10 g, 1.58×10^{-2} mol) were dissolved in anhydrous DMF (250 mL) under nitrogen and the solution was heated to 110 °C. The reaction was stirred for 3 days, during which time the reaction turned dark orange. The mixture was cooled to room temperature and poured into cold water (750 mL) containing 0.5 M of sodium hydroxide. The precipitate was filtered through a Büchner funnel, collected, and dissolved in chloroform. The chloroform solution was then extracted with deionized water; the organic layer was collected and dried over $MgSO_4$. After solvent evaporation, a brown oil was obtained and purified by column chromatography on silica (1:1 hexanes and methylene chloride) followed by recrystallization from ethanol and chloroform (2:3) to give 5.32 g (64%) of the product as a slightly yellow solid. Mp: 100−101 °C. ^{1}H NMR ($CDCl_3$): δ 6.92 (s, 1H), 3.98 (t, 2H), 3.71 (s, 2H), 1.80 (p, 2H), 1.43 (m, 2H), 1.28 (m, 16H), 0.89 (t, 3H). ^{13}C NMR ($CDCl_3$): δ 150.25, 119.31, 118.06, 112.85, 69.24, 32.14, 29.88, 29.85, 29.82, 29.79, 29.59, 29.57, 29.47, 26.28, 22.91, 18.87, 14.34. IR (KBr cm^{-1}) 2916, 2849, 2245, 1513, 1464, 1426, 1393, 1340, 1262, 1222, 1143, 1070, 1043, 999, 963, 923, 872, 846, 801, 759, 721. HRMS: calcd for $C_{34}H_{56}N_2O_2$, 524.4342; found, 524.4324. Anal. Calcd for $C_{34}H_{56}N_2O_2$: C, 77.81; H, 10.76; N, 5.34. Found: C, 77.62, H, 10.97; N, 5.06.

2,5-Bis(cyanomethyl)-1-methoxy-4-[(2-ethylhexyl)oxy]benzene (1b).[43] Same procedure as for compound **1a** with sodium cyanide (0.871 g, 1.78×10^{-2} mol, 2.5 equiv), 2,5-bis(bromomethyl)-1-methoxy-4-[(2-ethylhexyl)oxy]benzene (3 g, 7.11×10^{-3} mol) and anhydrous DMF (125 mL). The crude product was purified by column chromatography on silica (1:5 hexanes and methylene chloride) followed by recrystallization from hexanes to give 0.97 g (44%) of slightly yellow solid. Mp: 80−82 °C. ^{1}H NMR ($CDCl_3$): δ 6.94 (s, 1H), 6.93 (s, 1H), 3.88 (d, 2H), 3.86 (s, 3H), 3.71 (s, 4H), 1.75 (m, 1H), 1.3−1.6 (m, 8H), 0.94 (m, 6H). IR (KBr cm^{-1}) 3054, 2959, 2933, 2874, 2248, 1513, 1466, 1421, 1406, 1318, 1231, 1195, 1187, 1107, 1036, 983, 915, 882, 844, 759. HRMS: calcd for $C_{19}H_{26}N_2O_2$, 314.1994; found, 314.1994. Anal. Calcd for $C_{19}H_{26}N_2O_2$: C, 72.58; H, 8.33; N, 8.91. Found: C, 72.70, H, 8.40; N, 8.81.

1,4-Bis(cyanomethyl)-2-(3,7-dimethyloxy)-5-methoxybenzene (1c). Same procedure as for compound **1a** with sodium cyanide (4.0 g, 8.16×10^{-2} mol, 4.5 equiv), 1,4-bis(chloromethyl)-2-(3,7-dimethyloxy)-5-methoxybenzene (6.54 g, 1.81×10^{-2} mol) and anhydrous DMF (250 mL). The crude product was purified by column chromatography on silica (1:4 hexanes and dichloromethane) followed by recrystallization from hexanes to give 1.7 g (27%) of slightly yellow solid. Mp: 81−82 °C. ^{1}H NMR ($CDCl_3$): δ 6.93 (s, 2H), 4.02 (t, 2H), 3.86 (s, 3H), 3.71 (s, 4H), 1.84 (m, 1H), 1.5−1.7 (m, 5H), 1.1−1.4 (m, 4H), 0.96 (d, 3H), 0.88 (d, 6H). ^{13}C NMR ($CDCl_3$): δ 150.72, 150.40, 119.36, 119.22, 118.0, 112.89, 112.0, 67.57, 56.34, 39.44, 37.49, 36.42, 30.12, 28.20, 24.9, 22.92, 22.82, 19.90, 18.88, 18.34. IR (KBr cm^{-1}) 3054, 2953, 2927, 2870, 2248, 1517, 1467, 1422, 1407, 1317, 1231, 1188, 1155, 1030, 975, 916, 882, 760, 734. HRMS: calcd for $C_{21}H_{30}N_2O_2$, 342.2313; found, 342.2307. Anal. Calcd for $C_{21}H_{30}N_2O_2$: C, 73.65; H, 8.83; N, 8.18. Found: C, 73.87, H, 8.88; N, 8.04.

3,3-Bis(hexyloxy)-3,4-dihydro-2*H*-thieno-[3,4-*b*][1,4]-dioxepine [ProDOT($CH_2OC_6H_{13})_2$]. A 250 mL three-neck round-bottom flask equipped with a condenser, filled with anhydrous DMF (125 mL), 1-hexanol (2.23 g, 2.19×10^{-2} mol) and sodium hydride (1.06 g, 4.38×10^{-2} mol) was heated overnight at 110 °C. ProDOT-($CH_2Br)_2$ (2.5 g, 7.3×10^{-3} mol) was added and the reaction continued at 110 °C for another 48 h. After completion, the solution was cooled to room temperature, deionized water was added, and the mixture was extracted with diethyl ether. The ether layer was washed with brine and dried over $MgSO_4$. After filtration through a Büchner funnel, the solvent was evaporated, and a brown oil was collected. The crude product was purified by column chromatography on silica using chloroform as elution solvent to give 1.39 g (49%) of the product as a clear oil.^{1}H NMR ($CDCl_3$): δ 6.45 (s, 1H), 4.02 (s, 2H), 3.49 (s, 2H), 3.41 (t, 2H), 1.54 (p, 2H), 1.29 (m, 6H), 0.9 (t, 3H). ^{13}C NMR ($CDCl_3$): δ 149.93, 105.27, 73.97, 71.96, 69.79, 47.92, 31.88, 29.71, 26.02, 22.84, 14.27. HRMS: calcd for $C_{21}H_{36}O_4S$, 384.2334; found, 384.2322.

3,3-Bis(hexyloxy)-3,4-dihydro-2*H*-thieno-[3,4-*b*][1,4]dioxepine-6,8-dicarbaldehyde [ProDOT($CH_2OC_6H_{13})_2$($CHO)_2$] (2a). ProDOT($CH_2OC_6H_{13})_2$ (1.37 g, 3.98×10^{-3} mol) was dissolved in dry THF (40 mL) under nitrogen purge, and the solution was cooled to −78 °C. *n*-Butyllithium (2.5 equiv, 9.95×10^{-3} mol) was added via syringe, and the solution warmed to 0 °C for 30 min and then cooled back to −78 °C. Anhydrous DMF (1.5×10^{-2} mol, 3.8 equiv) was added rapidly via syringe, and the solution warmed to room temperature and stirred for 1 h. The solution was then poured into 3 M HCl and extracted with methylene chloride. The organic layer was washed with saturated $NaHCO_3$ and dried with $MgSO_4$. After filtration through Büchner funnel, the solvent was evaporated, and a brown oil collected. The crude product was purified by column chromatography on silica using ethyl acetate/hexanes (1/3) to collect 0.817 g (51%) of product as a yellow oil. ^{1}H NMR ($CDCl_3$): δ 9.98 (s, 1H), 4.19 (s, 2H), 3.46 (s, 2H), 3.37 (t, 2H), 1.56 (p, 2H), 1.23 (m, 6H), 0.82 (t, 3H). ^{13}C NMR ($CDCl_3$): δ 182.22, 155.04, 128.21, 74.91, 72.07, 69.54, 47.78, 31.83, 29.65, 26.01, 22.84, 14.26. IR (KBr cm^{-1}) 3317, 2931, 2859, 2734, 2660, 1667, 1559, 1489, 1466, 1436, 1376, 1306, 1249, 1194, 1103, 1065, 925, 833, 760, 727, 694, 552. HRMS: calcd for $C_{23}H_{36}O_6S$, 440.2233; found, 440.2236. Anal. Calcd for $C_{23}H_{36}O_6S$: C, 62.70; H, 8.24. Found: C, 63.06, H, 8.51.

3,3-Bis(2-ethylhexyloxymethyl)-3,4-dihydro-2*H*-thieno-[3,4-*b*]-[1,4]dioxepine-6,8-dicarbaldehyde [ProDOT($CH_2OEtHex)_2$-($CHO)_2$] (2b). Same procedure as for compound **2a** was use with ProDOT($CH_2OEtHex)_2$ (2.4 g, 5.44×10^{-3} mol), dry THF (40 mL), *n*-BuLi (2.3 equiv, 12.53×10^{-3} mol), dry DMF (3.7 equiv, 20.13×10^{-3} mol). Most of the impurities were removed from the crude product by column chromatography on silica (1:1, methylene chloride/hexanes); the product was then pushed out of the column with methylene chloride, decolorized with decolorizing carbon, and the rest of the impurities were removed by a second column chromatography on silica (1:2, ethyl acetate: hexanes) to yield 2.0 g (74%) of product as a yellow oil.^{1}H NMR ($CDCl_3$): δ 10.06 (s, 2H), 4.27 (s, 4H), 3.53 (s, 4H), 3.33 (d, 4H), 1.2−1.57 (m, 18H), 0.90 (m, 12H). ^{13}C NMR ($CDCl_3$): δ 182.20, 155.04, 128.13, 74.99, 74.60, 47.92, 339.79, 30.84, 29.31, 24.2, 23.28, 14.31, 11.35. IR (KBr cm^{-1}) 3318, 2958, 2928, 2859, 2734, 2661, 1666, 1559, 1489, 1460, 1436, 1376, 1307, 1248, 1193, 1103, 1064, 917, 833, 760, 728, 694, 552. HRMS: calcd for $C_{27}H_{44}O_6S$, 496.2859; found, 496.2859. Anal. Calcd for $C_{27}H_{44}O_6S$: C, 65.29; H, 8.93. Found: C, 65.47, H, 9.20.

PProDOT—OEtHex$_2$:CNPV—DDO. Compounds **2b** (0.5 g, 1×10^{-3} mol) and **1a** (0.525 g, 1×10^{-3} mol) were dissolved in a mixture of dry THF (42 mL) and freshly distilled *tert*-butyl alcohol (42 mL). Then, potassium *tert*-butoxide (0.224 g, 2×10^{-3} mol) was added, and the solution was heated to 70°C for 2 h. The color darkened progressively from yellow to blue to black. The solution was then cooled to room temperature and poured into ice cold methanol (600 mL) acidified with 1 mL of acetic acid. The resulting precipitate was isolated by filtration into a Soxhlet thimble and Soxhlet extracted for 48 h with methanol, and 24 h with chloroform. The solvent was evaporated from the chloroform fraction and a blue solid collected (0.6 g, 61%). ^{1}H NMR ($CDCl_3$, ppm): δ = 8.73 (b, 1H), 6.92 (b, 1H), 3.8−4.6 (bm, 6H), 3.2−3.8 (bm, 8H), 1.95 (b, 4H), 1−1.7 (bm, 34H), 0.92 (bm, 15H). IR (KBr cm^{-1}) 2958, 2924, 2854, 2205, 1640, 1574, 1512, 1475, 1448, 1378, 1282, 1181, 1142, 1069, 1026, 920, 861, 802. GPC analysis: M_n = 10 300, M_w = 14 800, PDI = 1.43. Anal. Calcd: C, 74.35; H, 10.06; N, 2.80; S, 3.20. Found: C, 64.87; H, 10.63; N, 2.11; S, 2.87.

PProDOT—OHex$_2$:CNPV—DDO. The same procedure as for **PProDOT—OEtHex$_2$:CNPV—DDO** was used with compound **2a** (0.427 g, 9.7×10^{-4} mol), compound **1a** (0.509 g, 9.7×10^{-4} mol), dry THF (39 mL), *tert*-butyl alcohol (39 mL), and potassium *tert*-butoxide (220 mg, 1.96×10^{-3} mol). During the polymerization, the solution color changed from yellow to black with a purple tint. After purification by Soxhlet extraction as above, 0.66 g (77%) of blue solid was collected. ^{1}H NMR ($CDCl_3$, ppm): δ = 8.70 (b, 1H), 6.90 (b, 1H), 3.8−4.7 (bm, 6H), 3.2−3.7 (bm, 8H), 1.93 (b, 2H), 1−1.7 (bm, 34H), 0.89 (bm, 9H). IR (KBr cm^{-1}) 2961, 2923, 2853, 2204, 1653, 1573, 1512, 1476, 1448, 1382, 1260, 1092, 1074, 1020, 862, 800, 706. GPC analysis: M_n = 13 100, M_w = 17 500, PDI = 1.34. Anal. Calcd: C, 73.68; H, 9.81; N, 2.96; S, 3.39. Found: C, 51.56; H, 9.56; N, 1.40; S, 1.74.

PProDOT—OHex$_2$:CNPV—MEH. The same procedure as for **PProDOT—OEtHex$_2$:CNPV—DDO** was used with compound **2a** (0.41 g, 9.3×10^{-4} mol), compound **1b** (0.32 g, 9.3×10^{-4} mol), THF (35 mL), *tert*-butyl alcohol (35 mL), and potassium *tert*-butoxide (210 mg, 1.87×10^{-3} mol). During the polymerization, the solution color changed from yellow to black. After purification by Soxhlet extraction as above, 0.286 g (41%) of purple solid was collected. ^{1}H NMR ($CDCl_3$, ppm): δ = 8.1−8.4 (b, 2H), 6.80−6.90 (b, 2H), 3.95−4.4 (bm, 9H), 3.45−3.95 (bm, 8H), 1.1−1.7 (bm, 25H), 0.89 (bm, 12H). IR (KBr cm^{-1}) 2955, 2925, 2858, 2205, 1647, 1578, 1505, 1476, 1445, 1378, 1281, 1261, 1217, 1100, 1067, 918, 868, 801. GPC analysis: M_n = 8700, M_w = 11 400, PDI = 1.31. Anal. Calcd: C, 70.26; H, 8.50; N, 3.81; S, 4.36. Found: C, 54.10; H, 7.60; N, 2.30; S, 3.04.

PProDOT—OHex$_2$:CNPV—MDMO. The same procedure as for PProDOT−OEtHex$_2$:CNPV−DDO was used with compound **2a** (0.45 g, 1.02×10^{-3} mol), compound **1c** (0.321 g, 1.02×10^{-3} mol), THF (35 mL), *tert*-butyl alcohol (35 mL), and potassium *tert*-butoxide (230 mg, 2.05×10^{-3} mol). During the polymerization, the solution color changed from yellow to black with a purple tint. After purification by Soxhlet extraction as above, 0.33 g (45%) of purple solid was collected. ^{1}H NMR ($CDCl_3$, ppm): δ = 8.1−8.4 (b, 2H), 6.90 (b, 2H), 3.9−4.45 (bm, 9H), 3.45−3.9 (bm, 8H), 1.2−1.88 (bm, 26H), 0.9 (bm, 12H). IR (KBr cm^{-1}) 2959, 2920, 2851, 2204, 1720, 1646, 1573, 1506, 1476, 1446, 1415, 1261, 1095, 1068, 1025, 862, 801. GPC analysis: M_n = 23 700, M_w = 31 100, PDI = 1.31. Anal. Calcd: C, 70.83; H, 8.72; N, 3.67; S, 4.20. Found: C, 62.44; H, 8.14; N, 2.97; S, 3.33.

Acknowledgment. This work was supported by grants from AFOSR (FA955-06-1-0192) and EIC (NASA−NNC05CB23C). We thank Dr. Gang Li (UCLA) for technical discussions.

Supporting Information Available: Text giving experimental information, including instrumentation information, figures and tables showing MALDI results, a figure showing the IR spectrum of PProDOT−OEtHex$_2$:CNPV−DDO, and figures showing GPC photodiode array detector measurements, TGA measurements, polymer CV and DPV results, thin-film optical absorbance spectra of the polymers in the neutral state, and IPCE results. This material is available free of charge via the Internet at http://pubs.acs.org.

References and Notes

(1) Shi, C.; Yao, Y.; Yang, Y.; Pei, Q. *J. Am. Chem. Soc.* **2006**, *128*, 8980−8986.
(2) Mozer, A. J.; Sariciftci, N. S. *C. R.. Chimie* **2006**, *9*, 568−577.
(3) Hou, J.; Tan, Z.; Yan, Y.; He, Y.; Yang, C.; Li, Y. *J. Am. Chem. Soc.* **2006**, *128*, 4911−4916.
(4) Kim, Y.; Cook, S.; Tuladhar, S. M.; Choulis, S. A.; Nelson, J.; Durrant, J. R.; Bradley, D. D. C.; Giles, M.; McCulloch, I.; Ha, C.-S.; Ree, M. *Nat. Mater.* **2006**, *5*, 197−203.
(5) Liu, M. S.; Niu, Y.-H.; Luo, J.; Chen, B.; Kim, T.-D.; Bardecker, J.; Jen, A. K.-Y. *Polym. Rev.* **2006**, *46*, 7−26.
(6) Liu, J.; Zhou, Q. G.; Cheng, Y. X.; Geng, Y. H.; Wang, L. X.; Ma, D. G.; Jing, X. B.; Wang, F. S. *Adv. Funct. Mater.* **2006**, *16*, 957−965.
(7) Zhang, X.; Chen, Z.; Yang, C.; Li, Z.; Zhang, K.; Yao, H.; Qin, J.; Chen, J.; Cao, Y. *Chem. Phys. Lett.* **2006**, *422*, 386-390.
(8) Reeves, B. D.; Grenier, C. R. G.; Argun, A. A.; Cirpan, A.; McCarley, T. D.; Reynolds, J. R. *Macromolecules* **2004**, *37*, 7559−7569.
(9) Argun, A. A.; Aubert, P.-H.; Thompson, B. C.; Schwendeman, I.; Gaupp, C. L.; Hwang, J.; Pinto, N. J.; Tanner, D. B.; MacDiarmid, A. G.; Reynolds, J. R. *Chem. Mater.* **2004**, *16*, 4401−4412.
(10) Sonmez, G. *Chem. Commun.* **2005**, *42*, 5251−5259.
(11) Mortimer, R. J.; Dyer, A. L.; Reynolds, J. R. *Displays* **2006**, *27*, 2−18.
(12) Zhu, Y.; Babel, A.; Jenekhe, S. A. *Macromolecules* **2005**, *38*, 7983−7991.
(13) Zhang, R.; Li, B.; lovu, M. C.; Jeffries-EL, M.; Sauvé, G.; Cooper, J.; Jia, S.; Tristram-Nagle, S.; Smilgies, D. M.; Lambeth, D. N.; McCullough, R. D.; Kowalewski, T. *J. Am. Chem. Soc.*. **2006**, *128*, 3480−3481.
(14) Ishikawa, T.; Fujita, K.; Tsutsui, T. *Jpn. J. Appl. Phys., Part 1: Reg. Pap., Brief Commun. Rev. Pap.* **2005**, *44*, 6292−6294.
(15) Shaheen, S. E.; Radspinner, R.; Peyghambarian, N.; Jabbour, G. E. *Appl. Phys. Lett.* **2001**, *79*, 2996−2998.
(16) Burns, S. E.; Cain, P.; Mills, J.; Wang, J.; Sirringhaus, H. *MRS Bull.* **2003**, *28*, 829−834.
(17) Liu, Y.; Cui, T. *Macromol. Rapid Commun.* **2005**, *26*, 289−292.
(18) Hay. M.; Klavetter, F. L. *J. Am. Chem. Soc.* **1995**, *117*, 7112−7118.
(19) Liu, B.; Yu, W.-L.; Lai, Y.-H.; Huang, W. *Chem. Mater.* **2001**, *13*, 1984−1991.
(20) Thomas, C. A.; Zong, K.; Abboud, K. A.; Steel, P. J.; Reynolds, J. R. *J. Am. Chem. Soc.* **2004**, *126*, 16440−16450.
(21) Walczak, R. M.; Cowart, J. S., Jr.; Abboud, K. A.; Reynolds, J. R. *Chem. Commun.* **2006**, *15*, 1604−1606.
(22) Yang, R.; Tian, R.; Yan, J.; Zhang, Y.; Yang, J.; Hou, Q.; Yang, W.; Zhang, C.; Cao, Y. *Macromolecules* **2005**, *38*, 244−253.
(23) Zhang, F.; Perzon, E.; Wang, X.; Mammo, W.; Andersson, M. R.; Inganäs, O. *Adv. Funct. Mater.* **2005**, *15*, 745−750.
(24) Xia, Y.; Luo, J.; Deng, X.; Li, X.; Li, D.; Zhu, X.; Yang, W.; Cao, Y. *Macromol. Chem. Phys.* **2006**, *207*, 511−520.
(25) Wienk, M. M.; Turbiez, M. G. R.; Struijk, M. P.; Fonrodona, M.; Janssen, R. A. J. *Appl. Phys. Lett.* **2006**, *88*, 153511.
(26) Arbizzani, C.; Catellani, M.; Mastragostino, M.; Mingazzini, C. *Electrochim. Acta* **1995**, *40*, 1871−1876.
(27) Arbizzani, C.; Cerroni, M. G.; Mastragostino, M. *Sol. Energy Mater. Sol. Cells* **1999**, *56*, 205−211.
(28) Du Bois, C. J., Jr.; Larmat, F.; Irvin, D. J.; Reynolds, J. R. *Synth. Met.* **2001**, *119*, 321−322.
(29) van Mullekom, H. A. M.; Vekemans, J. A. J. M.; Havinga, E. E.; Meijer, E. W. *Mater. Sci. Eng.* **2001**, *32*, 1−40.
(30) Wienk, M. J.; Struijk, Martin, P.; Janssen, R. A. J. *Chem. Phys. Lett.* **2006**, *422*, 488−491.
(31) Salzner, U. *Synth. Met.* **2001**, *119*, 215−216.
(32) Huang, H.; He, Q.; Lin, H.; Bai, F.; Cao, Y. *Thin Solid Films* **2005**, *477*, 7−13.
(33) Thompson, B. C.; Kim, Y.-G.; Reynolds, J. R. *Macromolecules* **2005**, *38*, 5359−5362.
(34) Thompson, B. C.; Kim, Y.-G.; McCarley, T. D.; Reynolds, J. R. *J. Am. Chem. Soc.* **2006**, *128*, 12714−12725.
(35) Coakley, K. M.; McGehee, M. D. *Chem. Mater.* **2004**, *16*, 4533−4542.
(36) Winder, C.; Sariciftci, N. S. *J. Mater. Chem.* **2004**, *14*, 1077−1086.
(37) de Leeuw, D. M.; Simenon, M. M. J.; Brown, A. R.; Einerhand, R. E. F. *Synth. Met.* **1997**, *87*, 53−59.
(38) Bard, A. J.; Faulkner, L. R. *Electrochemical Methods: Fundamentals and Applications*, 2nd ed.; Wiley: New York, 2001.
(39) Meskers, S. C. J.; Hübner, J.; Oestreich, M.; Bässler, H. *J. Phys. Chem. B* **2001**, *105*, 9139−9149.

(40) Cacialli, F.; Wilson, J. S.; Michels, J. J.; Daniel, C.; Silva, C.; Friend, R. H.; Severin, N.; Samori, P.; Rabe, J. P.; O'Connell, M. J.; Taylor, P. N.; Anderson, H. L. *Nat. Mater.* **2002**, *1*, 160−164.
(41) Alem, S.; de Bettignies, R.; Nunzi, J.-M. *Appl. Phys. Lett.* **2004**, *84*, 2178−2180.
(42) Padinger, F.; Fromherz, T. *Appl. Phys. Lett.* **2001**, *78*, 841−843.
(43) Li, X.-C.; Liu, Y.; Liu, M. S.; Jen, A. K.-Y. *Chem. Mater.* **1999**, *11*, 1568−1575.
(44) Neef, C. J.; Ferraris, J. P. *Macromolecules* **2000**, *33*, 2311−2314.
(45) Roex, H.; Adriaensens, P.; Vanderzande, D.; Gelan, J. *Macromolecules* **2003**, *36*, 5613−5622.
(46) Thompson, B. C. Variable band gap poly(3,4-alkylenedioxythiophene)-based polymers for photovoltaic and electrochromic applications, Ph.D. Dissertation, University of Florida, Gainesville, FL, 2005.
(47) Kricheldorf, H. R.; Schwartz, G. *Macromol. Rapid Commun.* **2003**, *24*, 359−381.
(48) Kricheldorf, H. R.; Fritsch, D.; Vakhtangishvili, L.; Schwartz, G. *Macromol. Chem. Phys.* **2005**, *206*, 2239−2247.
(49) Montaudo, G.; Montaudo, M. S.; Puglisi, C.; Samperi, F. *Rapid Commun. Mass Spectrom.* **1995**, *9*, 453−460.
(50) Axelsson, J.; Scrivener, E.; Haddleton, D. M.; Derrick, P. J. *Macromolecules* **1996**, *29*, 8875−8882.
(51) Schriemer, D. C.; Li, L. *Anal. Chem.* **1997**, *69*, 4169−4175.
(52) Du, H.; Fuh, R. A.; Li, J.; Corkan, A.; Lindsey, J. S. *Photochem. Photobiol.* **1998**, *68*, 141−142.
(53) Pavlishchuk, V. V.; Addison, A. W. *Inorg. Chim. Acta* **2000**, *298*, 97−102.
(54) Thompson, B. C.; Schottland, P.; Zong, K.; Reynolds, J. R. *Chem. Mater.* **2000**, *12*, 1563−1571.
(55) Ma, W.; Yang, C.; Gong, X.; Lee, K.; Heeger, A. J. *Adv. Funct. Mater.* **2005**, *15*, 1617−1622.
(56) Reyes-Reyes, M.; Kim, K.; Caroll, D. L. *Appl. Phys. Lett.* **2005**, *87*, 083506.
(57) Li, G.; Shrotriya, V.; Huang, J.; Yao, Y.; Moriarty, T.; Emery, K.; Yang, Y. *Nat. Mater.* **2005**, *4*, 864−868.
(58) Brinchi, L.; Germani, R.; Goracci, L.; Savelli, G.; Bunton, C. A. *Langmuir* **2002**, *18*, 7821−7825.

MA061935O